Infectious Disease Modelling 8 (2023) 656–671

Contents lists available at ScienceDirect

Infectious Disease Modelling

journal homepage: www.keaipublishing.com/idm

Time delay of the appearance of a new strain can affect vaccination behavior and disease dynamics: An evolutionary explanation

Md. Mamun-Ur-Rashid Khan [a, c, *], Md. Rajib Arefin [a, c], Jun Tanimoto [a, b]

[a] Interdisciplinary Graduate School of Engineering Sciences, Kyushu University, Kasuga-koen, Kasuga-shi, Fukuoka, 816-8580, Japan
[b] Faculty of Engineering Sciences, Kyushu University, Kasuga-koen, Kasuga-shi, Fukuoka, 816-8580, Japan
[c] Department of Mathematics, University of Dhaka, Dhaka, 1000, Bangladesh

ARTICLE INFO

Article history:
Received 8 November 2022
Received in revised form 26 March 2023
Accepted 5 June 2023
Available online 11 June 2023
Handling Editor: Dr Yijun Lou

Keywords:
Vaccination
Behavior dynamics
Two-strain epidemic
Time delay
Social efficiency deficit

ABSTRACT

The emergence of a novel strain during a pandemic, like the current COVID-19, is a major concern to the healthcare system. The most effective strategy to control this type of pandemic is vaccination. Many previous studies suggest that the existing vaccine may not be fully effective against the new strain. Additionally, the new strain's late arrival has a significant impact on the disease dynamics and vaccine coverage. Focusing on these issues, this study presents a two-strain epidemic model in which the new strain appears with a time delay. We considered two vaccination provisions, namely preinfection and post-infection vaccinations, which are governed by human behavioral dynamics. In such a framework, individuals have the option to commit vaccination before being infected with the first strain. Additionally, people who forgo vaccination and become infected with the first train have the chance to be vaccinated (after recovery) in an attempt to avoid infection from the second strain. However, a second strain can infect vaccinated and unvaccinated individuals. People may have additional opportunities to be vaccinated and to protect themselves from the second strain due to the time delay. Considering the cost of the vaccine, the severity of the new strain, and the vaccine's effectiveness, our results indicated that delaying the second strain decreases the peak size of the infected individuals. Finally, by estimating the social efficiency deficit, we discovered that the social dilemma for receiving immunization decreases with the delay in the arrival of the second strain.

1. Introduction

Multistrain infection models are essential tools for studying and predicting infection dynamics in the presence of many active strains. Many illnesses, including human immunodeficiency virus (HIV), dengue fever, tuberculosis (TB), and even the current COVID-19, can arise when two or more strains coexist. For example, H1N1 flu virus infection is considered a seasonal

* Corresponding author. Interdisciplinary Graduate School of Engineering Sciences, Kyushu University, Kasuga-koen, Kasuga-shi, Fukuoka, 816-8580, Japan.
E-mail address: mamun.math@du.ac.bd (Md.M.-U.-R. Khan).
Peer review under responsibility of KeAi Communications Co., Ltd.

https://doi.org/10.1016/j.idm.2023.06.001

influenza mutation, whereas COVID-19 is categorized as a novel SARS-CoV-1 strain. This mutation process can result in the emergence of new strains, especially if an effective medication has yet to be developed (Brenchley et al., 2006; Gorbalenya et al., 2020; Halstead, 2017). In the epidemic's propagation phase, the time it takes for a new strain to arise also plays a crucial role (Barro, Guiro, & Ouedraogo, 2018; Ma, Takeuchi, Hara, & Beretta, 2002; Xia, Kundu, & Maitra, 2018). In the meantime, the cost of immunization and the vaccine's efficiency against the new strain significantly influence worldwide epidemic dynamics (Ariful Kabir & Tanimoto, 2019; Dashtbali & Mirzaie, 2021; Deka & Bhattacharyya, 2022; Epstein, Hatna, & Crodelle, 2021; Rajib Arefin, Masaki, Ariful Kabir, & Tanimoto, 2019; Zuo, Zhu, Meng, et al., 2022).

Most compartmental models, which are a negotiable instrument in the study of disease transmission and well-being administration frameworks, are as often as possible utilized to look at any epidemic process or pandemic. The SIR model, designed by Kermack and Mckendrick, is the most extensively used epidemiological model (Ogilvy Kermack & McKendrick, 1927). It has been altogether investigated and extended to see an assortment of speculations and circumstances. Simply put, this show portrays how ailment voyages in individuals from the susceptible compartment (S) to the infected compartment (I) and after that to the recovered compartment (R), where individuals construct insusceptibility to reinfection. Exposed (E), quarantine (Q), hospitalized (H), and asymptomatic (A) compartments can be used in some epidemics to adequately examine disease dynamics (Ma et al., 2002; Barro et al., 2018; Xia et al., 2018; Epstein et al., 2021; Amador, Armesto, & Gómez-Corral, 2019; De León, Avila-Vales, & lin Huang, 2022; Amaral, Oliveira, & Javarone, 2021; Kabir, Risa, & Tanimoto, 2021; M. et al., 2005; Meskaf, Khyar, Danane, & Allali, 2020; Farah, Amine, & Allali, 2021; Dong, Li, Wan, & Liu, 2017; Li, Wang, Xu, & Rong, 2022; Khyar & Allali, 2020; Li, Liu, & Martcheva, 2010; Lazebnik & Bunimovich-Mendrazitsky, 2022; Beretta & Breda, 2011; Rihan, Alsakaji, & Rajivganthi, 2020; Khan, Ikram, Din, Humphries, & Akgul, 2021; Niño-Torres, Ríos-Gutiérrez, Arunachalam, Ohajunwa, & Seshaiyer, 2022; Zuo, Zhu, & Ling, 2022; Li & Liu, 2014). Examination of supervision and moderation measures, like immunization, establishing of vector-borne maladies, and the impact of birthing and passing elements is an extra application of compartmental models in the study of disease transmission (Dashtbali & Mirzaie, 2021; De León et al., 2022; Deka & Bhattacharyya, 2022; Epstein et al., 2021; Han & Li, 2022; Helbing et al., 2015; Jusup et al., 2022; Kabir et al., 2021; Lobinska, Pauzner, Traulsen, Pilpel, & Nowak, 2022; Nakata & Omori, 2015; Rajib Arefin et al., 2019; Tchoumi & Tchuenche, 2021; Tori & Tanimoto, 2022; Yin, Wang, Xia, & Bauch, 2022; Zuo, Zhu, & Ling, 2022). Misinformation dissemination, corruption, and resource misuse are factors that might be examined in SIR dynamics. However, most of these models focus on the evolution of the illness instead of the individual's behavioral response to the situation. However, numerous irresistible infection control approaches depend on human and organizational decision-making (Dashtbali & Mirzaie, 2021; Deka & Bhattacharyya, 2022; Kabir et al., 2021; Poletti, Caprile, Ajelli, Pugliese, & Merler, 2009; Rajib Arefin et al., 2019; Yin et al., 2022; Zuo et al., 2022a, 2022b). In, this context, the new field of behavioral epidemiology that incorporates psychology and game theory into epidemiology attracted significant attention (Agusto et al., 2022; Jusup et al., 2022; Kabir, 2021; Lobinska et al., 2022; Niño-Torres et al., 2022; Tanimoto, 2015, 2019, 2021). Individual behavior, rather than a static role, is considered in behavioral epidemiology. Sociophysics, a cutting-edge discipline that combines statistical physics with evolutionary game theory (EGT) to better explain human behavior, is the ideal discipline for this situation (Tanimoto, 2015, 2019, 2021; Tori & Tanimoto, 2022). Bauch combined the SIR model with EGT to study the vaccine decision-making dynamics in a novel approach (Bauch, 2005; Bauch & Bhattacharyya, 2012; Yin et al., 2022). Any individual can choose their immunization based on disease dynamics, vaccination cost, and vaccine effectiveness (Ariful Kabir & Tanimoto, 2019; Dashtbali & Mirzaie, 2021; De León et al., 2022; Deka & Bhattacharyya, 2022; Helbing et al., 2015; Li & Guo, 2022; Rajib Arefin et al., 2019; Tchoumi & Tchuenche, 2021; Yin et al., 2022; Zuo, Zhu, & Ling, 2022). This later evolved into the “vaccination game” concept (Amaral et al., 2021; Ariful Kabir & Tanimoto, 2019; Deka & Bhattacharyya, 2022; Han & Li, 2022; Jusup et al., 2022; Kabir, 2021; Rajib Arefin et al., 2019; Szolnoki & Perc, 2015; Tanimoto, 2019, 2021; Tchoumi & Tchuenche, 2021). As a result of this technique, several observations and predictions in vaccination operations have been made. However, compared to investigations of the dynamical behaviors of multistrain epidemic models with vaccination and time delays, early studies have received little attention. The dynamics of a two-strain epidemic model were studied in (Rajib Arefin et al., 2019; De León et al., 2022; M. et al., 2005; Meskaf et al., 2020; Farah et al., 2021; Li et al., 2022; Khyar & Allali, 2020; Li et al., 2010; Lazebnik & Bunimovich-Mendrazitsky, 2022; Tchoumi & Tchuenche, 2021; Yang, Chen, & Liu, 2016; Theprungsimankul, Junsank, Abdulloh, & Chinviriyasit, 2011; Khatua, Pal, & Kar, 2014; Allali & Amine, 2022; Li, Zhang, & Zhou, 2020). Epidemic models with time delay were studied in (Barro et al., 2018; Beretta & Breda, 2011; Dong et al., 2017; Farah et al., 2021; Ma et al., 2002; Nakata & Omori, 2015; Nastasi, Perrone, Taffara, & Vitanza, 2022; Yang et al., 2016; Yang & Zhang, 2012). Multistrain models with vaccination behaviors were studied in (Rajib Arefin et al., 2019; Zuo, Zhu, Meng, et al., 2022; De León et al., 2022; Zuo, Zhu, & Ling, 2022; M. et al., 2005; Yin et al., 2022; Han & Li, 2022; Tchoumi & Tchuenche, 2021; Yang & Zhang, 2012). Stability analysis of multistrain models was found in (Allali & Amine, 2022; Dong et al., 2017; Farah et al., 2021; Khatua et al., 2014; Khyar & Allali, 2020; Meskaf et al., 2020; Tchoumi & Tchuenche, 2021; Tiwari, Rai, Khajanchi, Gupta, & Misra, 2021; Yang & Zhang, 2012).

Here, we propose an epidemic model with two-strain in which the first strain is active from the start of the disease and the second strain emerges after a while. People can be vaccinated in one of two ways: before they become infected with strain 1 or after recovering from it. The new strain can infect vaccinated and unvaccinated individuals. When people's preferred alternatives are to take a vaccination or not, as well as when to take a vaccine, the behavior model gives a framework for describing individual behavior. We also demonstrated the impact of the new strain's introduction on disease dynamics and individual vaccination behavior, as well as the total vaccine coverage considering the time delay. The concept of social efficiency deficit (SED), which is the difference between Nash equilibrium (NE) and the social optimum, is incorporated into our model (SO), to

generate a social dilemma, taking into account the vaccine's efficacy and cost (Ariful Kabir & Tanimoto, 2019; Kabir et al., 2021; Tori & Tanimoto, 2022; Tanimoto, 2019; Tanimoto, 2015; Tanimoto, 2021; Arefin, Kabir, Jusup, Ito, & Tanimoto, 2020; Huang, Wang, & Xia, 2020; wang & Xia, 2020; Khan, Arefin, & Tanimoto, 2022a; Khan, Arefin, & Tanimoto, 2022b).

2. Model formulation

2.1. Epidemic model

Here we suggest a nine-compartmental two-strain epidemiological model based on the SVIR (susceptible, vaccination, infectious, recovered) dynamics. We also introduce two behaviors: preinfection and postinfection vaccinations of individuals. Depiction of the proposed model is shown in Fig. 1. The formulation of the model is given as follows:

$$\dot{S} = -xS - \beta_1 S\left(I_1 + I_1^V\right) - \beta_2 S I_2 H \tag{1}$$

$$\dot{V}_1 = xS - \beta_1(1-e_1)\left(I_1 + I_1^V\right)V_1 - \beta_2(1-e_2)I_2 H V_1 \tag{2}$$

$$\dot{V}_2 = yR_1 - \beta_2(1-e_2)I_2 H V_2 \tag{3}$$

$$\dot{I}_1 = \beta_1 S\left(I_1 + I_1^V\right) - \gamma_1 I_1 - \varepsilon_1 H I_1 \tag{4}$$

$$\dot{I}_1^V = \beta_1(1-e_1)\left(I_1 + I_1^V\right)V_1 - \gamma_1 I_1^V - \varepsilon_2 H I_1^V \tag{5}$$

$$\dot{I}_2 = \beta_2 S I_2 H + \beta_2(1-e_2)I_2 H V_1 + \beta_2(1-e_2)I_2 H V_2 + \varepsilon_1 I_1 + \varepsilon_2 I_1^V + \beta_2 R_1 I_2 H + \beta_2(1-e_2)R_1^V I_2 H - \gamma_2 I_2 H \tag{6}$$

$$\dot{R}_1 = \gamma_1 I_1 - yR_1 - \beta_2 R_1 I_2 H \tag{7}$$

$$\dot{R}_1^V = \gamma_1 I_1^V - \beta_2(1-e_2)R_1^V I_2 H \tag{8}$$

$$\dot{R}_2 = \gamma_2 I_2 H \tag{9}$$

$$H(t-T) = \begin{cases} 0, t < T \\ 1, t \geq T \end{cases}, \mathrm{T} = \text{time delay of the appearence of strain 2} \tag{10}$$

$$S(t) + V_1(t) + V_2(t) + I_1(t) + I_1^V(t) + I_2(t) + R_1(t) + R_1^V(t) + R_2(t) = 1 \tag{11}$$

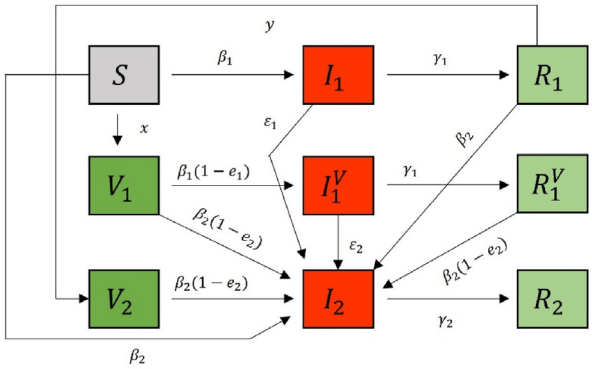

Fig. 1. Depiction of the proposed model.

where $S, V_1, V_2, I_1, I_1^V, I_2, R_1, R_1^V,$ and R_2 are the fractions of individuals of susceptible, preinfected vaccinated, postinfected vaccinated, nonvaccinated and infected with strain 1, vaccinated and infected with strain 1, infected with strain 2, nonvaccinated and recovered from strain 1, vaccinated and recovered from strain 1, and recovered from strain 2, respectively. The total population is normalized to 1. Initially, every people are considered as susceptible. Individuals can choose vaccination and can move to the compartment V_1. Both the susceptible and vaccinated people can be infected with strain 1 since strain 1 is effective from the initial time of disease spreading. Those people who are not vaccinated at the first stage but got infected can take the vaccination after recovery from the strain 1 infection and can move to the V_2 compartment. In our study, we have considered a single type of vaccine whose efficiency is already known against the first strain but different for the second strain. All the vaccinated and nonvaccinated individuals can be infected by strain 2 when it appears. The Heaviside function $H(t-T)$ is used to control the time delay of the appearance of strain 2. β_1 and β_2 are the transmission rates of strain 1 and strain 2 respectively. We consider $\beta_1 < \beta_2$ because the new strain is highly transmissible (Farah et al., 2021; Khyar & Allali, 2020). We also demonstrate the dynamics for the opposite scenario. γ_1 and γ_2 are the recovery rates from strain 1 and strain 2 respectively. Additionally, we consider $\gamma_1 > \gamma_2$, i.e., the recovery time for strain 2 is higher (Farah et al., 2021; Khyar & Allali, 2020). e_1 and e_2 are the vaccine efficacy values for strain 1 and strain 2, respectively. We have taken into account the fixed efficacy of the vaccine for strain 1, but we vary the efficacy for the new strain to demonstrate the vaccination behavior and the social dilemma. ε_1 and ε_2 are the mutation rates from nonvaccinated strain 1 and vaccinated strain 1 to strain 2, respectively. We have considered a very low mutation rate from strain 1 to strain 2. T represents the time delay of the emergence of strain 2. We didn't consider any co-infection of strain 1 and strain 2 in our work (Allali & Amine, 2022; Khyar & Allali, 2020; Rajib Arefin et al., 2019; Tchoumi & Tchuenche, 2021). Table 1 presents all parameters and their meaning.

2.2. Behavior model

We discuss the idea of the behavior model, which explains the flux changing throughout time from susceptible (S) to preinfection vaccination (V_1) denoted by x and from the infected but recovered from strain 1 (R_1) to postinfected vaccination (V_2) denoted by y (Bauch, 2005; Bauch & Bhattacharyya, 2012; Yin et al., 2022). We illustrate the following two dynamical equations:

$$\dot{x} = t_x\, x\,(1-x)\left\{c_i\left(m_1 I_1 + m_1 I_1^V + m_2 I_2 H\right) - k\, c\right\} \tag{12}$$

$$\dot{y} = t_y\, y\,(1-y)\{c_i m_2 I_2 H - k\, c\} \tag{13}$$

where t_x and t_y are the inertial effects for the rate of the vaccinations; c_i and c are the disease cost and vaccination cost, respectively; m_1 and m_2 are the severity effects of strain 1 and 2, respectively; and k is the relative sensitivity to taking the vaccination due to its cost. We have considered $c_i = 1.0$ throughout our study. Most earlier models included the total number of infected people at any given time, the cost of the disease, and the cost of vaccination when calculating the dynamics of vaccines (Kabir et al., 2021; Tori & Tanimoto, 2022). The severity effect m_1, m_2 of the strains is considered in our study with the other parameters. The new strain frequently appears to be more severe and highly transmissible in most cases, such as the current COVID-19. To assess the dynamics of vaccination, the severity effect is also a crucial parameter. For the preinfection vaccination, we considered all infected individuals at any given time in equation (12). However, for the postinfection vaccination, we only take into account the total population of individuals infected with strain 2 in equation (13). This is because individuals who did not receive the vaccine the first time may be persuaded to do so by the emergence of a highly contagious and more severe strain.

Table 1
Model parameters and their description.

Parameters	Description
β_1	Rate of strain 1's disease transmission
β_2	Rate of strain 2's disease transmission
e_1	Efficacy of the vaccine to strain 1
e_2	Efficacy of the vaccine to strain 2
γ_1	Recovery proportion for strain 1
γ_2	Recovery proportion for strain 2
ε_1	Mutation rate from strain 1 to strain 2 for nonvaccinated
ε_2	Mutation rate from strain 1 to strain 2 for vaccinated
t_x	Inertial effect on preinfection vaccination
t_y	Inertial effect on postinfection vaccination
m_1	Severity effect of strain 1
m_2	Severity effect of strain 2
c_i	Disease cost
c	Vaccination cost
k	Relative sensitivity due to the cost of vaccination

2.3. Primary reproduction number

We calculated the primary reproduction numbers for both strains using the next-generation matrix approach (Arruda, Das, Dias, & Pastore, 2021; Li et al., 2010; Martcheva, 2009, 2013). For this, by considering the infection equations (4)–(6), we have

$$\mathscr{F} = \begin{pmatrix} \beta_1 S I_1 + \beta_1 S I_1^V \\ \beta_1 V_1(1-e_1) I_1 + \beta_1 V_1(1-e_1) I_1^V \\ \left(\varepsilon_1 I_1 + \varepsilon_2 I_1^V + \left(\beta_2 S + \beta_2(1-e_2)V_2 + \beta_2 R_1 + \beta_2(1-e_2)R_1^V + \beta_2(1-e_2)V_1\right) I_2\right) H \end{pmatrix}$$

$$\nu = \begin{pmatrix} (\gamma_1 + \varepsilon_1 H) I_1 \\ (\gamma_1 + \varepsilon_2 H) I_1^V \\ \gamma_2 I_2 H \end{pmatrix}$$

Then, from $\mathscr{F}$ and ν, we calculate the matrices as follows:

$$F = \begin{pmatrix} \beta_1 S & \beta_1 S & 0 \\ \beta_1 V_1(1-e_1) & \beta_1 V_1(1-e_1) & 0 \\ \varepsilon_1 H & \varepsilon_2 H & \left(\beta_2 S + \beta_2(1-e_2)V_2 + \beta_2 R_1 + \beta_2(1-e_2)R_1^V + \beta_2(1-e_2)V_1\right) H \end{pmatrix}$$

$$V = \begin{pmatrix} \gamma_1 + \varepsilon_1 H & 0 & 0 \\ 0 & \gamma_1 + \varepsilon_2 H & 0 \\ 0 & 0 & \gamma_2 H \end{pmatrix}$$

$$V^{-1} = \begin{pmatrix} \frac{1}{\gamma_1 + \varepsilon_1 H} & 0 & 0 \\ 0 & \frac{1}{\gamma_1 + \varepsilon_2 H} & 0 \\ 0 & 0 & \frac{1}{\gamma_2 H} \end{pmatrix}$$

Then, the next-generation matrix becomes,

$$M = FV^{-1} = \begin{pmatrix} \frac{\beta_1 S}{\gamma_1 + \varepsilon_1 H} & \frac{\beta_1 S}{\gamma_1 + \varepsilon_2 H} & 0 \\ \frac{\beta_1 V_1(1-e_1)}{\gamma_1 + \varepsilon_1 H} & \frac{\beta_1 V_1(1-e_1)}{\gamma_1 + \varepsilon_2 H} & 0 \\ \frac{\varepsilon_1 H}{\gamma_1 + \varepsilon_1 H} & \frac{\varepsilon_2 H}{\gamma_1 + \varepsilon_2 H} & \frac{\left(\beta_2 S + \beta_2(1-e_2)V_2 + \beta_2 R_1 + \beta_2(1-e_2)R_1^V + \beta_2(1-e_2)V_1\right) H}{\gamma_2 H} \end{pmatrix}$$

Finally, by calculating the eigenvalues of the matrix M, we have the following expressions for the primary reproduction number of strains 1 and 2.

$$R_{o1} = \frac{\beta_1 S}{\gamma_1 + \varepsilon_1 H} + \frac{\beta_1 V_1(1-e_1)}{\gamma_1 + \varepsilon_2 H} \tag{14}$$

$$R_{o2} = \frac{\left(\beta_2 S + \beta_2(1-e_2)V_2 + \beta_2 R_1 + \beta_2(1-e_2)R_1^V + \beta_2(1-e_2)V_1\right)}{\gamma_2} \tag{15}$$

2.4. Final epidemic size (FES), average social payoff (ASP), and social efficiency deficit (SED)

In this study, we calculated the FES in three ways (Yang & Zhang, 2012): FES of only strain 1 (*FESOS*1), FES of only strain 2 (*FESOS*2), and FES of both strains (*FESBoth*). The expressions for the FESs are defined as follows:

$$FESOS1 = R_1(\infty) + V_2(\infty) \tag{16}$$

$$FESOS2 = \int_{t=0}^{\infty} (\beta_2 S I_2 H + \beta_2 (1-e_2) V_1 I_2 H)\, dt \tag{17}$$

$$FESBoth = \int_{t=0}^{\infty} \left(\beta_2 R_1 I_2 H + \beta_2 (1-e_2) V_2 I_2 H + \beta_2 (1-e_2) R_1^V I_2 H + \varepsilon_1 I_1 H + \varepsilon_2 I_1^V H\right) dt \tag{18}$$

where the symbol ∞ denotes a state of equilibrium (let's name it NE) at $t = \infty$.

The vaccination coverages preinfected v_x and postinfected v_y and the total vaccination coverage v_c are defined as

$$v_x = \int_{t=0}^{\infty} xS\, dt \tag{19}$$

$$v_y = \int_{t=0}^{\infty} yR_1\, dt \tag{20}$$

Then,

$$v_c = v_x + v_y \tag{21}$$

The average social payoff (ASP^{NE} in the model can be defined as follows:

$$ASPNE = c_i\, (FESOS1 + FESOS2 + 2\, FESBoth) - c\, v_c \tag{22}$$

where the first item on the right-hand side represents the overall disease cost when combining the affected individuals with either one strain or both strains, and the second term represents the entire vaccine cost. Individuals' disease cost for each strain c_i is taken as 1.0 in this the study. Those afflicted with both strains must pay twice the disease cost.

By referring to the original SED idea (Arefin et al., 2020), which evaluates the discrepancy between ASP at NE and ASP at SO to determine whether a social dilemma underlies in the current social-dynamical system or not. If the x and y evolutionary processes are properly controlled, SED demonstrates how to increase the system's ASP from an evolutionary final state (NE) to a hypothetical perfect society to attain the highest ASPSO imaginable. It is defined as follows:

$$SED = ASPSO - ASPNE \tag{23}$$

The social optimal state is a time-constant vector $(x\ (for\ SO), y\ (for\ SO))$, with both elements in the range $[0, 1]$. Thus, we have

$$\boldsymbol{SO} = \text{argmax}\, [ASP(x\ (for\ SO), y\ (for\ SO))] \tag{24}$$

When NE agrees with SO, SED implies zero. Meanwhile, when SED is positive but not zero, there is a social dilemma.

3. Results and discussions

3.1. Standard (Basic) case

The time series graph for the proposed model employing the common (basic) parameters set is shown in Fig. 2(a). The initial value for the compartments and vaccination rates, as well as the common values for the parameters, are shown in Tables 2 and 3 respectively. We considered that the transmission rate of strain 1 (β_1) is lower than the transmission rate of strain 2 (β_2). We also considered the efficacy of the vaccine for strain 1 (e_1) is higher than the efficacy of the vaccine for strain 2 (e_2). The mutation rates $\varepsilon_1, \varepsilon_2$ from strain 1 to strain 2 were taken quite low. In the standard case, we considered the appearance of strain 2 after $T = 60$ days after the appearance of strain 1. Fig. 2(b) shows that the transmission rate of strain 2 is lower than that of strain 1 (reversing the values of β_1 and β_2), with all the remaining parameters, kept the same.

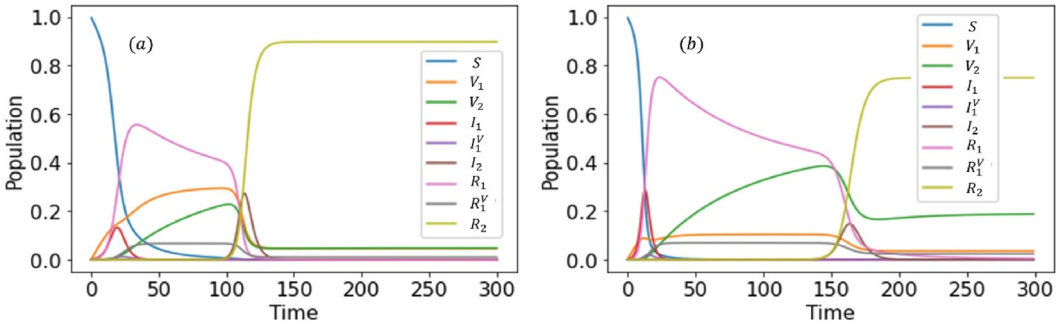

Fig. 2. Time series of the compartments for a common case. Here, the blue line indicates the susceptible people; the orange and green lines indicate the vaccinated people before and after being infected with strain 1, respectively; red, violet and brown indicate the infected people with strain 1 (nonvaccinated and vaccinated, respectively) and strain 2; pink and gray indicate the recovered people infected with strain 1 (nonvaccinated and vaccinated, respectively); and yellow indicates the recovered people infected with strain 2. In Fig. 2(a), the peak infection for strain 1 is approximately 0.15 and the peak infection for strain 2 is approximately 0.3. However, in Fig. 2(b), the peak infection for strain 1 is approximately 0.3 whereas the peak infection of strain 2 is approximately 0.15. In Fig. 2(a), almost 90% of the people are infected with strain 2 because the transmission rate of strain 2 is higher. However, in Fig. 2(b), nearly 80% of the people are infected with strain 2 because the transmission rate of strain 2 is lower.

Table 2
Values of the parameters (common case).

Parameter	Value	Parameter	Value
β_1	0.7	$\varepsilon_1, \varepsilon_2$	0.0001
β_2	1.0	t_x, t_y	1.0
e_1	0.7	m_1, m_2	1.0
e_2	0.5	c_i	1.0
γ_1	0.33	c	0.1
γ_2	0.25	k	0.1

Table 3
Initial values for the compartments and vaccination rate.

State	At $t = 0$	State/Rate	At $t = 0$
S	0.997	I_2	0.00
V_1	0.001	R_1	0.00
V_2	0.00	R_1^V	0.00
I_1	0.001	R_2	0.00
I_1^V	0.001	x, y	0.01

3.2. Time delay effect on primary reproduction number, R_o

Fig. 3 shows the time delay effect on Primary reproduction numbers R_{o1} and R_{o2}. We considered four cases. The appearance of strain 2 happens after $T = 1, 60, 120,$ and 240 days. For strain 1, the primary reproduction number always starts from the same point, approximately 2.2, and decreases with time. However, for strain 2, the starting point for the primary reproduction number decreases with time. Thus, if strain 2 appears at $T = 1$ days, i.e., almost simultaneous with strain 1, the initial value of the primary reproduction number starts from approximately 4.0 because strain 2 has a larger transmission rate. If the time delay for strain 2 is 60 days, the initial value of the primary reproduction number is approximately 3.1. Similarly, for $T = 120, 240$, the initial value of the primary reproduction number starts from 2.9 to 2.8 and decreases with the spent time.

3.3. Time delay effect on infection and vaccination

Fig. 4 shows the infection and vaccination time series using four distinct time delays of strain 2 emergence. The total infection for strain 1 (vaccinated and nonvaccinated) is shown in panel (a). We can see that the total infection of strain 1 is unaffected because of the time delay in the appearance of strain 2. The total infection peak is the same for $T = 1, 60, 120, 240$ (approximately 0.15). Infection for strain 2 is displayed in panel (b) showing that the infection peak decreases when the arrival of strain 2 is delayed. When $T = 1$ day, i.e., both strains are active practically concurrently from the start, the infection peak for strain 2 is the highest (approximately 0.35). However, when $T = 60, 120, 240$, the infection peaks for strain 2 are 0.28, 0.25, and 0.23, respectively. Panel (c) is made up of panels (a) and (b). As shown in these panels, the delay in the appearance of

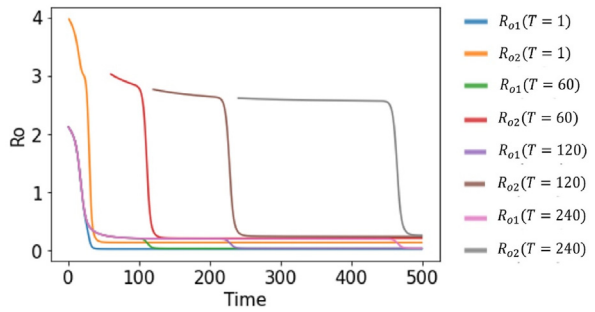

Fig. 3. Time series of primary reproduction numbers with different time delays of the appearance of strain 2. The values of the parameters are the same as those for the standard case. For strain 1, the starting points of R_{o1} is the same with different T values and they decrease with the spent time. However, the starting points of R_{o2} decrease with the delayed appearance of strain 2 and decrease with time.

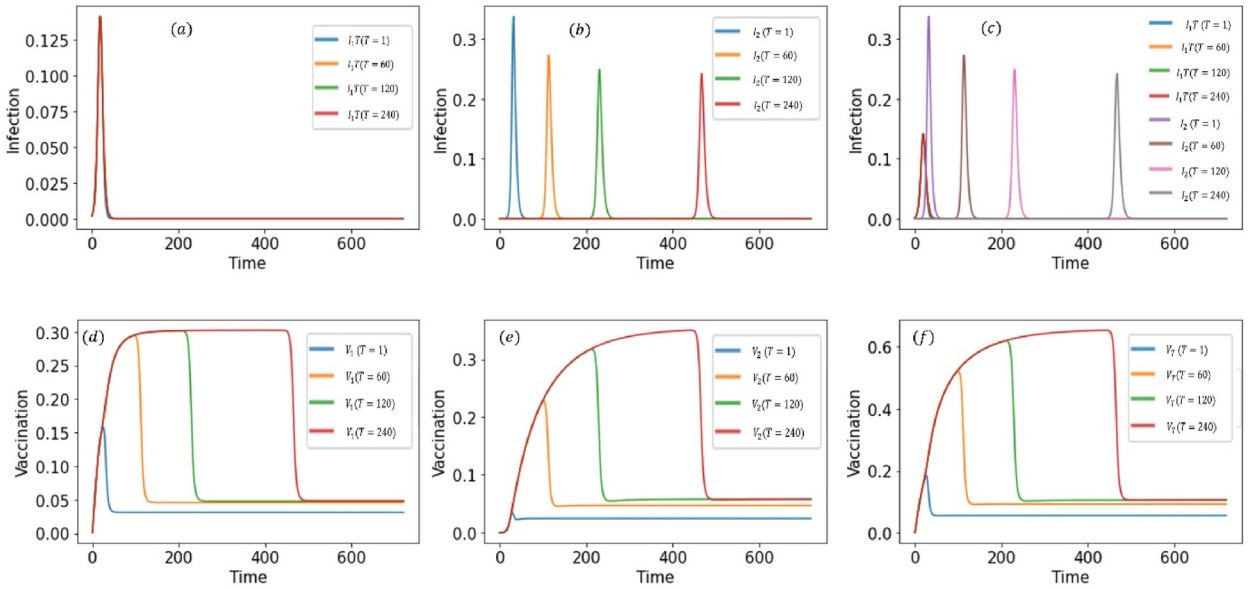

Fig. 4. Time series of infection and vaccination with a time delay of the appearance of strain 2. Panel (a) shows the total infection (I_1T) due to strain 1, and panel (b) shows the total infection due to strain 2 (I_2). Both (a) and (b) show the four different time delays of the appearance of strain 2. Panel (c) is the combination of (a) and (b). Panel (d) – (f) represent the time series of preinfected vaccinated (V_1), postinfected vaccinated (V_2), and total vaccinated (V_T), respectively. Here, time delay T is taken as $1, 60, 120, 240$ days and all parameters and initial values are kept the same as those of the standard case. We can observe from the panels that the time delay of the appearance can give people more chances to be vaccinated and can reduce the risk of infection from strain 2.

strain 2 does not affect the infection of strain 1 but it does diminish the peak size of strain 2, implying that strain 2 becomes weaker as time passes.

Preinfection, postinfection, and entire vaccination time series are illustrated in panels (d), (e), and (f). If $T = 1$, there is less time for vaccination instead of infection in panel (d). If $T = 60, 120, 240$ persons have time to be vaccinated, approximately 30% of them (vaccination peak always occurs approximately 0.3) received their vaccination before becoming sick with any strain. In panel (e), the vaccination peak increases as the arrival of strain 2 is delayed. After being infected with strain 1 for $T = 240$, over 35% of persons (peaking at approximately 0.35) can be vaccinated. The entire vaccination time series is presented in panel (f). We can see that delaying the appearance of strain 2 increases the possibility of postinfection vaccination and hence overall vaccination, lowering the risk of infection with strain 2, which is complementary to panels (a) – (c).

3.4. Time delay and inertial effects on vaccination

Fig. 5 shows the inertial and time delay effects on vaccination. Here, we considered three time delays $T = 60, 120, 240$ and three sets of inertial effects $(t_x, t_y) = (0.1, 0.1), (0.5, 0.5), (1.0, 1.0)$ on vaccination. For $T = 60$, panels (a) – (c) show the time series of preinfection vaccination, postinfection vaccination, and total vaccination. In panel (a), we can observe that preinfection vaccination is less with the less inertial effect and it is high with maximum inertial effect. This is obvious when the

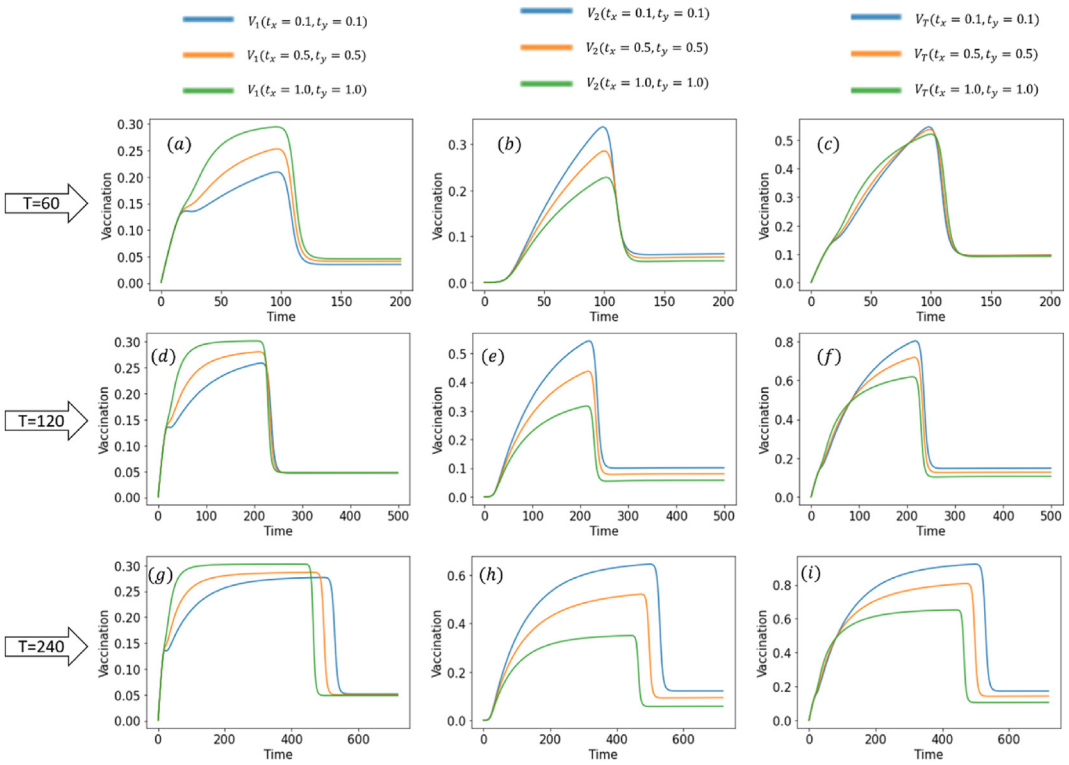

Fig. 5. Time series of preinfected vaccinated (V_1), postinfected vaccinated (V_2), and total vaccinated (V_T) people are presented with three sets of inertial effect $(t_x, t_y) = (0.1, 0.1), (0.5, 0.5), (1.0, 1.0)$ along with $T = 60, 120, 240$ days. The remaining parameters are taken as standard ones. These figures show that the time delay of the emergence of the second strain can help people be vaccinated more and less inertial effect can increase the total number of vaccinated people as a whole.

high inertial effect is active, i.e., people giving maximum effort, the preinfected vaccinees is maximum. However, the behavior of postinfection vaccination is the opposite. We can see from panel (b), that a less inertial effect gives maximum vaccines whereas a high inertial effect gives fewer vaccines. This is because with a high inertial effect, most people take the vaccine before they are infected with strain 1 and fewer people who can take the vaccine after being infected with strain 1 remain. Meanwhile, if fewer people take the vaccine earlier (when the less inertial effect has been considered), there will be more people remaining, who can be infected with strain 1 and can take the vaccine to become safe from strain 2. A combination of (a) and (b) shows in panel (c), that the total vaccination looks similar, but for the less inertial effect the peak of the total vaccination seems higher.

For $T = 120$, panels (d) – (f) are displayed. In panel (d), we can see similar behavior on preinfection vaccination time series like panel (a) which means that less inertial effect implies fewer people choose vaccination before being infected with strain 1. In panel (e), similar behavior is observed like panel (b), less inertial effect implies more people take the vaccine after being infected with strain 1. However, the infection peaks in all three cases in panel (e) are much higher than the corresponding peaks in panel (b). Consequently, the combination of panels (d) and (e) i.e., panel (f), shows that the total vaccination peaks are also much higher than those in panel (c). This is because the time delay of the appearance of strain 2 gives much time to the people who are not vaccinated before being infected with strain 1. These people can take a vaccine when strain 2 emerges or is present.

For $T = 240$, panels (g) – (i) look almost similar to the corresponding panels (d)– (f). However, peaks in panels (h) and(i) are higher than the corresponding peaks of panels (e) and (f) because of the time delay of the appearance of strain 2. Thus, we can see that the time delay of the appearance of strain 2 can increase the chance of taking a vaccine, which can reduce the risk of infection. Additionally, a less inertial effect may help make more people vaccinated.

3.5. Time delay and severity effects on vaccination

Fig. 6 shows the severity and time delay effects of vaccination. Here, we considered three-time delays $T = 60, 120, 240$, and three sets of severity effect $(m_1, m_2) = (0.1, 0.1), (0.5, 0.5), (1.0, 1.0)$ on vaccination. For $T = 60$, panels (a) – (c) show the time series of preinfected vaccination, postinfected vaccination, and total vaccination. In panel (a), we observed that the vaccination peak is highest when the severity effect is maximum. This is obvious because if the severity is higher for any

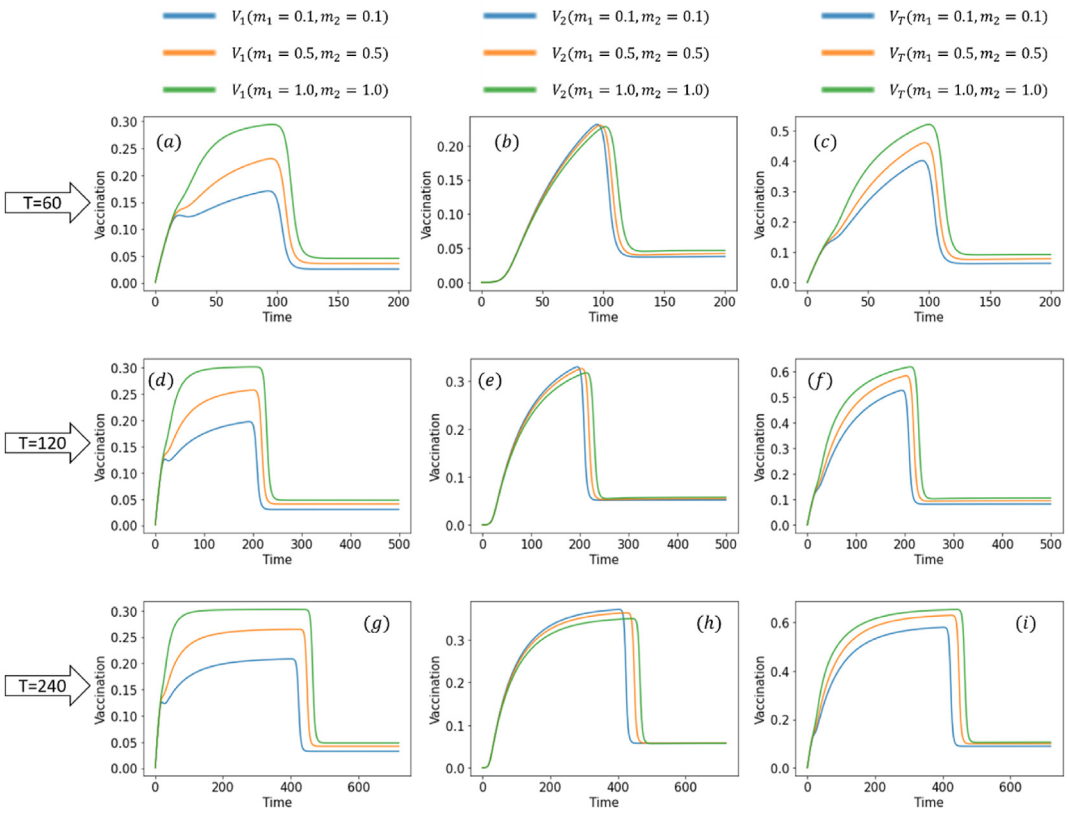

Fig. 6. Time series of preinfected vaccinated (V_1), postinfected vaccinated (V_2), and total vaccinated (V_T) people are presented with three sets of severity effects $(m_1, m_2) = (0.1, 0.1), (0.5, 0.5), (1.0, 1.0)$ along with $T = 60, 120, 240$ days. The remaining parameters are taken as standard ones. These figures, show that the time delay of the emergence of a second strain can help people be vaccinated more and a higher severity effect can also increase the total number of vaccinated people.

strain, people must go for the vaccination as early as it is available. In panel (b), we observed almost a similar behavior with different severity effects because after being infected with strain 1, every person tries to take the vaccination to remain safer from strain 2. Panel (c) is the combination of panels (a) and (b), which reflects that more severity implies more vaccination.

For $T = 120$, panels (d) – (f) have similar behavior corresponding to panels (a)– (c). In panel (d), the peaks of the vaccination compared to panel (a) are similar, but in panel (e), peaks are much higher than those in panel (b). This is because the time delay of the appearance of strain 2 gives more time for people to be vaccinated. Consequently, panel (f) shows that the peak of the total vaccinated people is higher than that in panel (c).

For $T = 240$, panels (g) – (i) also behave similarly compared to panels (d)– (f). However, the postinfection vaccination peak is a little higher in panels (h) and (i) than in panels (e) and (f) because of the time delay of the appearance of strain 2. Therefore these panels show that more severe diseases can increase the chance of vaccination and more time delay increases the chance of vaccination, which can reduce the risk of infection.

3.6. Time delay effect on ASP and SED

In this subsection, We investigate the impact of the time delay on the ASP and SED to observe the social dilemma of the proposed model. We also considered four distinct time delay effects: $T = 1, 60, 120, 240$. Heatmaps were created using the vaccine's cost c as the x-axis and its effectiveness e_2 to strain 2 as the y-axis.

Fig. 7.1 shows the heatmaps of the final epidemic sizes for only strain 1, only strain 2, both strains, vaccination coverage, and the average social payoff for NE and SO cases, as well as the SED for the time delay $T = 1$, i.e., both strains almost effective for the entire time. The situation for NE is depicted in panels (a) – (e), whereas the case for SO is depicted in panels (f)– (j). SED is depicted in panel (k) with the difference between (j) and (e). To explain the general context of the case, we divided the SED region into two different regions (panel (k)).

When the efficacy is high and the cost of vaccination is low, we may see a light red corner in the left upper region in panel (a) in the NE case. The remaining region is dark red, indicating that when the efficacy is high and the cost is low, only a small percentage of the population will remain infected with only strain 1. When the efficacy is high and the cost is low, a dark red

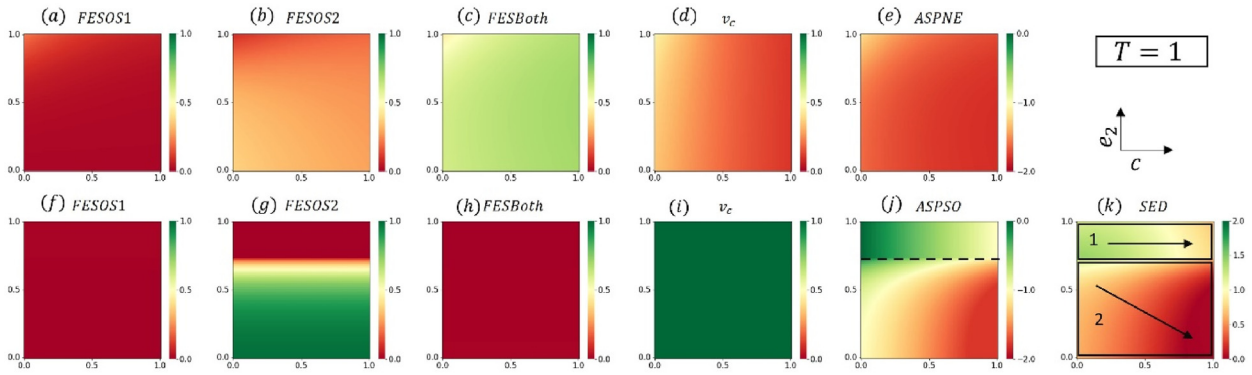

Fig. 7.1. This graph shows the FESs, vaccination coverage, ASP, and SED. For NE cases (panels (a) – (e)), the final epidemic sizes for only strain 1, only strain 2, both strains, vaccination coverage, and average social payoff are shown in the first row, whereas the instances for SO are shown in the second row (panels (f)– (j). SED is depicted in panel (k). The cost of the vaccination c is plotted on the x-axis, whereas the efficacy of the vaccine e_2 against strain 2 is plotted on the y-axis, both ranging from 0 to 1. Except for these two, all other settings are set to their default values. The ranges of the FESs and vaccine coverage are taken from 0 to 1. The ASP panels range is taken from – 2.0 to 0.0 and the SED panel is depicted with a range from 0.0 to 2.0. At approximately $e_2 = 0.75$, a critical line is detected for the SO case, dividing the SED region into two sections. The arrival of strain 2 is given a time delay of $T = 1$ day.

region appears in the left upper region in panel (b), indicating that only a small percentage of people will be infected with only strain 2. When the time delay for strain 2 is 1 day, panel (c) shows that more than 50% of people will be infected with both strains. Panel (d) shows very little vaccination coverage for this case. Panel (e) illustrates the average social reward for the NE case when all of these panels ((a) – (d)) are combined. We can see that the average social payoff is low when the vaccination cost is low and the efficacy is high. We can also observe that in the SO situation, there are nearly no persons (panel (f)) who become infected with only strain 1, and vaccine coverage is at its highest (panel (i)). Additionally, there is a critical line between the value $e_2 = 0.75$ (panel (g)). No one will be infected with solely strain 2 beyond this critical line, and people will be infected with strain 2 below the line because of the vaccines' reduced efficiency against strain 2. Furthermore, the SO predicted that no one would be infected by both strains (panel (h)). Consequently, in the SO, the average social payoff produces two zones separated by the critical line. SED is shown in panel (k) with the difference between panels (j) and (e). The critical line separates regions (1) and (2) in the context of SED. We found a monotonic decline in the value of SED along the direction of vaccination cost in the region (1) (green to yellow). As the cost of vaccination increases, people will opt out. Similar behavior can be seen in region 2. However, the monotonic reduction occurs (light red to dark red) in the diagonal direction, implying that when vaccine efficacy is poor and vaccination costs are high, no one will be vaccinated. Thus, raising the price of less effective vaccines does not create a broader social dilemma.

Fig. 7.2 shows the case when the time delay, $T = 60$ days. Similar to the panels in Fig. 7.1, all panels are depicted with the same values of the parameters. Here, we can see that a triangular (green and yellow) region occurs in the upper left corner in panel (a), representing the FES of only strain 1. This means that with the high efficacy of strain 2, the low cost of the vaccine,

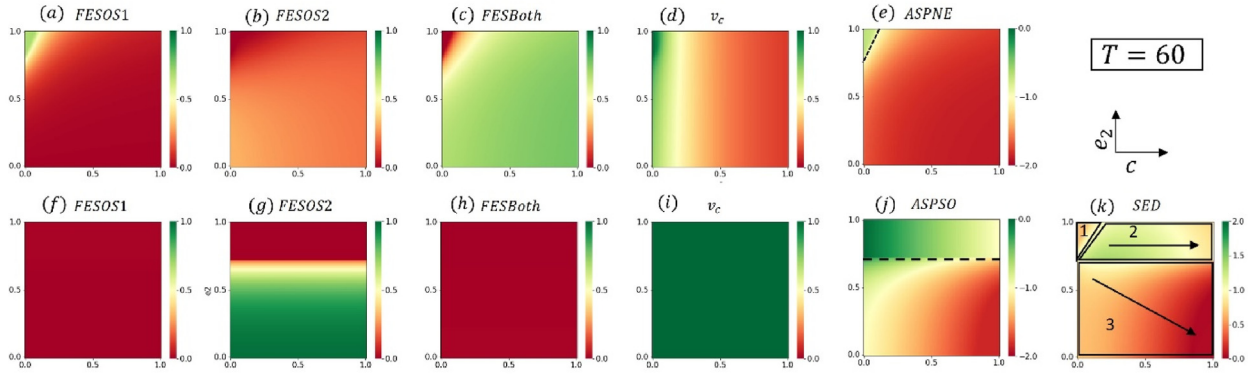

Fig. 7.2. This graph shows the FESs, vaccination coverage, ASP, and SED. For the NE case (panels (a) – (e)), the first row shows the final epidemic sizes for only strain 1, only strain 2, both strains, vaccination coverage, and average social payoff whereas, the second row (panels (f)– (j) shows the instances of SO. The SED was depicted in panel (k). The cost of the vaccination c is plotted on the x-axis, whereas the efficacy of the vaccine e_2 against strain 2 is plotted on the y-axis both ranging from 0 to 1. Except for these two, all other settings are set to their default values. The ranges of the FESs and vaccine coverage are taken from 0 to 1. The ASP panels range is taken from – 2.0 to 0.0 and the SED panel is depicted with a range from 0.0 to 2.0. At approximately $e_2 = 0.75$, a critical line is detected for the SO case and combined with the triangular region in the NE case, dividing the SED region into three sections. The arrival of strain 2 is given a time delay of $T = 60$ days.

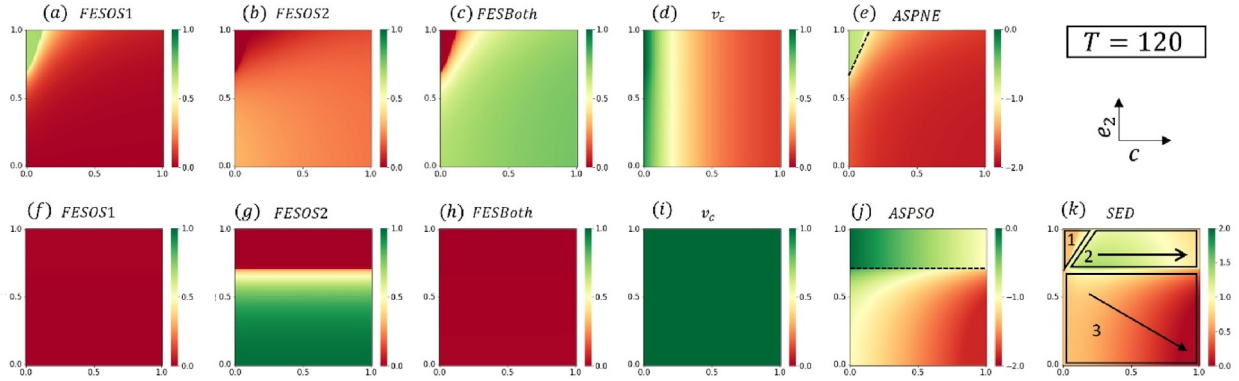

Fig. 7.3. This graph shows the FESs, vaccination coverage, ASP, and SED. The final epidemic sizes for only strain 1, only strain 2, both strains, vaccination coverage, and average social payoff are shown in the first row for NE (panels (a) – (e)), whereas the examples for SO are shown in the second row (panels (f)– (j)). The SED was depicted in panel (k). The cost of vaccination c is plotted, on the x-axis, whereas the efficacy of the vaccine e_2 against strain 2 is plotted on the y-axis, both ranging from 0 to 1. All other parameters, except for these two, are left at their default values. FESs and vaccination coverage are measured on a scale of 0–1. The ASP panels range from – 2.0 to 0.0, whereas the SED panel range from 0.0 to 2.0. For the SO case, a critical line is discovered at approximately $e_2 = 0.75$, dividing the SED region into three halves with the triangular region in NE. The arrival of strain 2 is given a time delay of $T = 120$ days.

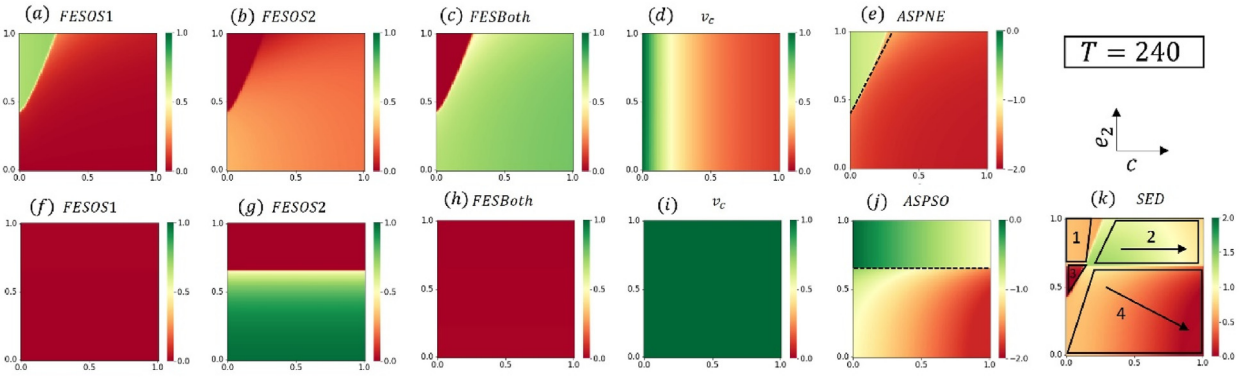

Fig. 7.4. This graph shows the FESs, vaccination coverage, ASP, and SED. In the first row for NE (panels (a) – (e)), the final epidemic sizes for only strain 1, only strain 2, both strains, vaccination coverage, and average social payoff are provided, whereas the examples for SO are shown in the second row (panels (f)–(j)). Panel (k) depicts the SED. The cost of vaccination c is plotted on the x-axis, whereas the efficacy of the vaccine e_2 against strain 2 is plotted on the y-axis, with both values ranging from 0 to 1. Except for these two, all other parameters are left at their default levels. FESs and vaccination coverage are rated on a scale of 0–1. The ASP panels range from – 2.0 to 0.0, while the SED panel range from 0.0 to 2.0. For the SO case, a critical line is discovered at approximately $e_2 = 0.75$, dividing the SED region into four parts, with the triangular region in NE. The arrival of strain 2 is given a time delay of $T = 240$ days.

and delayed appearance, some people have the chance not to be infected with strain 2. The dark red region of panels (b) and (c) compliments the scenario of the panel (a). In panel (d), with low cost and high efficacy, we see that most people go for vaccination because they also have 60 days to become vaccinated. As a combination of panels (a) – (d), panel (e) presented the ASP for the NE case where the ASP is lower in the left upper triangular region, i.e., people will take a vaccine rather than be infected with strain 2. In SO (panels (f)– (j)), similar behaviors are observed in Fig. 7.2, like in Fig. 7.1. SO suggested maximum vaccination, which also shows that no person will remain infected with only strain 1. We also observed a triangular region in SED (panel (k)) due to the triangular region occurring in the ASP at the NE. Therefore we divide the SED region into three parts using the observed critical line (panel (j)). Region 1 is light red because when the efficacy is high and the cost is low, most people will go for the vaccination and there will be a very less social dilemma. In region 2, increasing the cost of the vaccination decreases the social dilemma monotonically because as the price increases, people will not go for the vaccination. In region 3, the monotonic decreasing behavior is observed diagonally, as shown in Fig. 7.1. This implies that with low efficacy and high cost, people will lose interest in taking the vaccine and the social dilemma also decreases monotonically.

Fig. 7.3 depicts the situation where the time delay, $T = 120$ days. All panels are depicted with identical parameter values as those of the panels in Figs. 7.1 and 7.2. In panel (a), we can also see a triangle (green and yellow) zone in the left upper corner. This represents the FES of only strain 1, implying that owing to the vaccine's great efficiency against strain 2, low cost, and delayed appearance, some people may avoid becoming infected with strain 2. The triangular region of the panel (a) in Fig. 7.3 is slightly larger than that of panel (a) in Fig. 7.2, indicating that with an additional 60-day time delay, reduced efficacy, and a higher cost may be appropriate to avoid infection with strain 2. Panels (b) and (c) have a dark red section that matches the

scene in panel (a). Additionally, vaccine coverage in panel (d) of Fig. 7.3 is higher than that of panel (d) in Fig. 7.2, indicating that an extra 60 days can vaccinate more people. Panel (e), which contains a similar triangular green region when the vaccination cost is low and efficacy is high, is the average social payoff for the NE when panels (a) – (d) are combined. Fig. 7.3 shows comparable features to Figs. 7.1 and 7.2 in the SO (panels (f) – (j)). The SO for the maximum vaccination has been proposed, demonstrating that no one will remain infected with only strain 1. The critical line is also visible, indicating that if the vaccine efficiency is greater than 0.75, no one will be infected with strain 2. We have seen triangular and trapezium-shaped regions in SED (panel (k)) above the critical line because of the triangular region in the ASP at the NE and the critical line in the SO (panel (j)). Consequently, we partition the SED region into three regions using the observed critical line. Region 1 is light red because when vaccination efficiency is high and the cost is low, most people will opt for it and there will be less social dilemma. In region 2, increasing the cost of vaccination reduces the social problem monotonically because people will not be vaccinated as the price rises. In region 3, as shown in Figs. 7.1 and 7.2, the monotonic declining behavior is exhibited diagonally, indicating that with low efficacy and high cost, people will lose interest in taking the vaccine and the social dilemma will also diminish monotonically.

Fig. 7.4 shows the time delay $T = 240$ days. All of these panels are depicted with identical parameter values to the panels in Fig. 7.1– 7.3. A triangle (green and yellow) zone in the left upper corner of the panel (a) indicates the FES of only strain 1, indicating that some people may escape becoming infected with strain 2 due to the vaccine's high efficacy against strain 2, low cost, and delayed appearance. The triangular region of panel (a) in Fig. 7.4 is much larger than that of panel (a) in Fig. 7.3, showing that avoiding infection with strain 2 may be possible with an extra 120-day time delay but at a higher cost. A dark red portion appears in panels (b) and (c), corresponding to the scene in panel (a). Vaccine coverage in panel (d) of Fig. 7.4 is greater than that in panel (d) of Fig. 7.3, showing that an extra 120 days can vaccinate more people. It also exhibits a monotonically declining vaccine coverage with increasing vaccination costs, but less sensitivity with increasing vaccine efficacy. When panels (a) – (d) are merged, the average social payoff for the NE is panel (e), which has a comparable triangular green zone when the vaccine cost is low and efficacy is high. Fig. 7.4 in SO (panels (f)-(j)) has aspects that are similar to Figs. 7.1-7.3 in SO. It has been proposed that the SO for maximum vaccination is established, proving that no one will remain infected with only strain 1. The critical line, which indicates that no one will be infected with strain 2 if the vaccine efficacy is greater than 0.7, is also apparent. Because of the triangular region in the ASP at the NE and the critical line in SO, there are two trapezium-shaped regions in SED (panel (k)) above the critical line and one triangular and one trapezium-shaped region below the critical line. Consequently, we use the critical line to divide the SED region into four portions. When vaccine efficiency is high and the cost is cheap, most people will choose it and there will be fewer social dilemmas. In region 2, increasing the cost of vaccination lessens the social problem over time because people will refuse to be vaccinated as the cost increases. A dark red triangular section appears in region 3, indicating almost no dilemma issue. Using a $T = 240$-days time delay, some people may need to be vaccinated with a vaccine that is less expensive and has a lower efficiency (approximately 0.5). The monotonic falling behavior is displayed diagonally in region 4, as illustrated in Fig. 7.1–7.3, which means that with low efficacy and high cost, people will lose interest in taking the vaccine, and the social dilemma will also reduce monotonically.

4. Conclusion

The emergence of new strains creates a new challenge to the healthcare system. However, the time lag between the appearances of the resident and new strains can be substantially influential in determining the disease dynamics, especially for the second strain. Although vaccine efficacy against the new strain may reduce, its late appearance increases the possibility of higher vaccination coverage, inevitably reducing the infection peak (as well as epidemic size) concerning the new strain. This study investigated such a context by employing a two-strain epidemic model with preinection and postinfection vaccinations. More precisely, individuals who forgo vaccination and are infected with the resident strain have the chance to be vaccinated after recovery. As vaccination is mostly voluntary, we consider behavioral dynamics to model individuals' vaccination behavior. The decision to be vaccinated is influenced by the timing of the emergence of the new strain, its severity, transmission rate, and the cost and effectiveness of the vaccine. Most previous studies concerning two-strain or multi-strain epidemic models focused on stability analysis with non-monotone incidence rates, complex network with latency, general incidence rate, age structure and mutation (Allali & Amine, 2022; Meskaf et al., 2020; Yang et al., 2016; Yang & Zhang, 2012), competitive coexistence with periodic infection rate (Li et al., 2020), optimal control with general incidence function and time delay, imperfect vaccination, covid-19 application (Arruda et al., 2021; Barro et al., 2018; Li & Guo, 2022), vaccination behavior with imitation dynamic approach, social distance effect, covid-19 modeling, awareness decay (Dashtbali & Mirzaie, 2021; De León et al., 2022; Deka & Bhattacharyya, 2022; Zuo, Zhu, & Ling, 2022), and disease dynamics with cross-immunity, in patchy environments, generic approach (Amador et al., 2019; Lazebnik & Bunimovich-Mendrazitsky, 2022; Li et al., 2022; Theprungsimankul et al., 2011), etc.

Our primary concern was to observe the effect of vaccination and the time delay of the emergence of a new strain on controlling disease spreading. We have considered four-time delays of the appearance of new strains which has a huge impact on global disease dynamics and vaccination behavior which is not discussed in any other prior studies. Generally, vaccination is effective in reducing the disease spreading. We also demonstrated that the time delay of the advent of a new strain could considerably reduce the corresponding basic reproduction number. Our results further suggest that the larger the time delay is, the higher the vaccination coverage, reducing the peak and the final epidemic size of the new strain. In terms of the cost

and efficacy of the vaccine, we observed that higher efficacy and a lower cost increase vaccination uptake, which is quite comprehensible.

Later, we presented the SED analysis of our model which showed how the social dilemma situation acts with the emergence of new strain along with time delay. We found that SED, measured by the difference between the average payoff at the SO and equilibrium, can be reduced by vaccination and the increase in time delay. Our findings imply that vaccination and time delay are substantial in reducing SED. The lesser SED demonstrates that the evolutionary outcomes are closer to the SO. Also, as the time delay rises, we can see from Figs. 7.1–7.4 that the SED regions can be separated into additional sections to describe the social dilemma with various costs and levels of efficacy, which is a little bit intriguing.

In our model, we merely used a straightforward ODE model (mean-field approximation) technique to study the dynamics of vaccination behavior and social dilemma, and the social context lends credibility to our data. In future studies, we will investigate the result multiagent simulation approach. We will also include a single vaccination in our model with varying efficacy for the different strains. Furthermore, we will strive to expand our approach to include different vaccinations at various price points in addition to multidose vaccination. We considered the constant time delay of the appearance of a new strain in our work. Next, we will focus on how a time-variant time delay can affect disease dynamics, vaccination behavior, and social dilemma in our future study.

Funding

This study was partially supported by Grant-in-Aid for Scientific Research from JSPS, Japan, KAKENHI (Grant No. JP 19KK0262, JP 20H02314, and JP 20K21062) awarded to Professor Tanimoto. We would like to express our gratitude to them.

Intellectual property

We confirm that we have given due consideration to the protection of intellectual property associated with this work and that there are no impediments to publication, including the timing of publication, with respect to intellectual property. In so doing we confirm that we have followed the regulations of our institutions concerning intellectual property.

Research ethics

We further confirm that any aspect of the work covered in this manuscript that has involved human patients has been conducted with the ethical approval of all relevant bodies and that such approvals are acknowledged within the manuscript.

IRB approval was obtained (required for studies and series of 3 or more cases)

Written consent to publish potentially identifying information, such as details or the case and photographs, was obtained from the patient(s) or their legal guardian(s).

Authorship

All listed authors meet the ICMJE criteria.

We attest that all authors contributed significantly to the creation of this manuscript, each having fulfilled criteria as established by the ICMJE.

We confirm that the manuscript has been read and approved by all named authors.

We confirm that the order of authors listed in the manuscript has been approved by all named authors.

Declaration of competing interest

No conflict of interest exists.

Acknowledgments

This study was partially supported by Grant-in-Aid for Scientific Research from JSPS, Japan, KAKENHI (Grant No. JP 19KK0262, JP 20H02314, and JP 20K21062) awarded to Professor Tanimoto. We would like to express our gratitude to them.

References

wang, Z., & Xia, C. (2020). Co-evolution spreading of multiple information and epidemics on two-layered networks under the influence of mass media. *Nonlinear Dynamics, 102*, 3039–3051. https://doi.org/10.1007/s11071-020-06021-7

Agusto, F. B., Erovenko, I. V., Fulk, A., Abu-Saymeh, Q., Romero-Alvarez, D., Ponce, J., et al. (2022). To isolate or not to isolate: The impact of changing behavior on COVID-19 transmission. *BMC Public Health, 22*. https://doi.org/10.1186/s12889-021-12275-6, 1–20.

Allali, S., & Amine, A. (2022). Stability analysis of a fractional-order two-strain epidemic model with general incidence rates. *Commun. Math. Biol. Neurosci., 43*. https://doi.org/10.28919/cmbn/7297

Amador, J., Armesto, D., & Gómez-Corral, A. (2019). Extreme values in SIR epidemic models with two strains and cross-immunity. *Mathematical Biosciences and Engineering, 16*, 1992–2022. https://doi.org/10.3934/mbe.2019098

Amaral, M. A., Oliveira, M. M.d., & Javarone, M. A. (2021). An epidemiological model with voluntary quarantine strategies governed by evolutionary game dynamics. *Chaos, Solitons & Fractals, 143*, Article 110616. https://doi.org/10.1016/j.chaos.2020.110616
Arefin, M. R., Kabir, K. M. A., Jusup, M., Ito, H., & Tanimoto, J. (2020). Social efficiency deficit deciphers social dilemmas. *Scientific Reports, 10*, 1–9. https://doi.org/10.1038/s41598-020-72971-y
Ariful Kabir, K. M., & Tanimoto, J. (2019). Modelling and analysing the coexistence of dual dilemmas in the proactive vaccination game and retroactive treatment game in epidemic viral dynamics. *Proc. R. Soc. A Math. Phys. Eng. Sci., 475*. https://doi.org/10.1098/rspa.2019.0484
Arruda, E. F., Das, S. S., Dias, C. M., & Pastore, D. H. (2021). Modelling and optimal control of multi strain epidemics, with application to COVID-19. *PLoS One, 16*, 1–18. https://doi.org/10.1371/journal.pone.0257512
Barro, M., Guiro, A., & Ouedraogo, D. (2018). Optimal control of a SIR epidemic model with general incidence function and a time delays. *Cubo, 20*, 53–66. https://doi.org/10.4067/s0719-06462018000200053
Bauch, C. T. (2005). Imitation dynamics predict vaccinating behaviour. *Proc. R. Soc. B Biol. Sci., 272*, 1669–1675. https://doi.org/10.1098/rspb.2005.3153
Bauch, C. T., & Bhattacharyya, S. (2012). Evolutionary game theory and social learning can determine how vaccine scares unfold. *PLoS Computational Biology, 8*. https://doi.org/10.1371/journal.pcbi.1002452
Beretta, E., & Breda, D. (2011). An SEIR epidemic model with constant latency time and infectious period. *Mathematical Biosciences and Engineering, 8*, 931–952. https://doi.org/10.3934/mbe.2011.8.931
Brenchley, J. M., Price, D. A., Schacker, T. W., Asher, T. E., Silvestri, G., Rao, S., et al. (2006). Microbial translocation is a cause of systemic immune activation in chronic HIV infection. *Nature Medicine, 12*, 1365–1371. https://doi.org/10.1038/nm1511
Dashtbali, M., & Mirzaie, M. (2021). A compartmental model that predicts the effect of social distancing and vaccination on controlling COVID-19. *Scientific Reports, 11*, 1–11. https://doi.org/10.1038/s41598-021-86873-0
De León, U. A. P., Avila-Vales, E., & lin Huang, K. (2022). Modeling COVID-19 dynamic using a two-strain model with vaccination. *Chaos, Solitons & Fractals, 157*, Article 111927. https://doi.org/10.1016/j.chaos.2022.111927
Deka, A., & Bhattacharyya, S. (2022). The effect of human vaccination behaviour on strain competition in an infectious disease: An imitation dynamic approach. *Theoretical Population Biology, 143*, 62–76. https://doi.org/10.1016/j.tpb.2021.12.001
Dong, J., Li, T., Wan, C., & Liu, X. (2017). The analysis of a SEIRS epidemic model with time delay on complex networks. *OALib, 4*, 1–10. https://doi.org/10.4236/oalib.1103901
Epstein, J. M., Hatna, E., & Crodelle, J. (2021). Triple contagion: A two-fears epidemic model. *Journal of the Royal Society Interface, 18*. https://doi.org/10.1098/rsif.2021.0186
Farah, E. M., Amine, S., & Allali, K. (2021). Dynamics of a time-delayed two-strain epidemic model with general incidence rates. *Chaos, Solitons & Fractals, 153*, Article 111527. https://doi.org/10.1016/j.chaos.2021.111527
Gorbalenya, A. E., Baker, S. C., Baric, R. S., de Groot, R. J., Drosten, C., Gulyaeva, A. A., et al. (2020). The species severe acute respiratory syndrome-related coronavirus: Classifying 2019-nCoV and naming it SARS-CoV-2. *Nature Microbiology, 5*, 536–544. https://doi.org/10.1038/s41564-020-0695-z
Halstead, S. M. (2017). Dengue and dengue hemorrhagic fever, handb. Zoonoses, second Ed. *Sect. B Viral Zoonoses, 11*, 89–99. https://doi.org/10.1201/9780203752463
Han, D., & Li, X. (2022). On Evolutionary vaccination game in activity-driven networks. *IEEE Transactions on Computational Social Systems*, 1–11. https://doi.org/10.1109/TCSS.2021.3137724
Helbing, D., Brockmann, D., Chadefaux, T., Donnay, K., Blanke, U., Woolley-Meza, O., et al. (2015). *Saving human lives: What complexity science and information systems can contribute*. https://doi.org/10.1007/s10955-014-1024-9
Huang, J., Wang, J., & Xia, C. (2020). Role of vaccine efficacy in the vaccination behavior under myopic update rule on complex networks. *Chaos, Solitons & Fractals, 130*. https://doi.org/10.1016/j.chaos.2019.109425
Jusup, M., Holme, P., Kanazawa, K., Takayasu, M., Romić, I., Wang, Z., et al. (2022). Social physics. *Physics Reports, 948*, 1–148. https://doi.org/10.1016/j.physrep.2021.10.005
Kabir, K. M. A. (2021). How evolutionary game could solve the human vaccine dilemma. *Chaos, Solitons & Fractals, 152*, Article 111459. https://doi.org/10.1016/j.chaos.2021.111459
Kabir, K. M. A., Risa, T., & Tanimoto, J. (2021). Prosocial behavior of wearing a mask during an epidemic: An evolutionary explanation. *Scientific Reports, 11*, 1–14. https://doi.org/10.1038/s41598-021-92094-2
Khan, M. M. U. R., Arefin, M. R., & Tanimoto, J. (2022a). Investigating the trade-off between self-quarantine and forced quarantine provisions to control an epidemic: An evolutionary approach. *Applied Mathematics and Computation, 432*, Article 127365. https://doi.org/10.1016/j.amc.2022.127365
Khan, M. M. U. R., Arefin, M. R., & Tanimoto, J. (2022b). Investigating vaccination behavior and disease dynamics of a time-delayed two-strain epidemic model : An evolutionary approach. *Proceeding of International Exchange Innovation Conference on Engineering Science, 8*, 147–154.
Khan, A., Ikram, R., Din, A., Humphries, U. W., & Akgul, A. (2021). Stochastic COVID-19 SEIQ epidemic model with time-delay. *Results in Physics, 30*, Article 104775. https://doi.org/10.1016/j.rinp.2021.104775
Khatua, A., Pal, D., & Kar, T. K. (2014). Global dynamics of an epidemic model with a non-monotonic incidence rate. *Iran Journal of Science and Iranian Journal of Science and Technology, Transaction Science, 10*, 71–77. https://doi.org/10.9790/5728-10277177
Khyar, O., & Allali, K. (2020). Global dynamics of a multi-strain SEIR epidemic model with general incidence rates: Application to COVID-19 pandemic. *Nonlinear Dynamics, 102*, 489–509. https://doi.org/10.1007/s11071-020-05929-4
Lazebnik, T., & Bunimovich-Mendrazitsky, S. (2022). Generic approach for mathematical model of multi-strain pandemics. *PLoS One, 17*, 1–20. https://doi.org/10.1371/journal.pone.0260683
Li, T., & Guo, Y. (2022). Modeling and optimal control of mutated COVID-19 (Delta strain) with imperfect vaccination. *Chaos, Solitons & Fractals, 156*. https://doi.org/10.1016/j.chaos.2022.111825
Li, M., & Liu, X. (2014). An SIR epidemic model with time delay and general nonlinear incidence rate. *Abstract and Applied Analysis, 2014*. https://doi.org/10.1155/2014/131257
Li, X. Z., Liu, J. X., & Martcheva, M. (2010). An age-structured two-strain epidemic model with super-infection. *Mathematical Biosciences and Engineering, 7*, 123–147. https://doi.org/10.3934/mbe.2010.7.123
Li, C., Wang, J., Xu, J., & Rong, Y. (2022). The Global dynamics of a SIR model considering competitions among multiple strains in patchy environments. *Mathematical Biosciences and Engineering, 19*, 4690–4702. https://doi.org/10.3934/mbe.2022218
Li, C., Zhang, Y., & Zhou, Y. (2020). Competitive coexistence in a two-strain epidemic model with a periodic infection rate. *Discrete Dynamics in Nature and Society, 2020*. https://doi.org/10.1155/2020/7541861
Lobinska, G., Pauzner, A., Traulsen, A., Pilpel, Y., & Nowak, M. A. (2022). Evolution of resistance to COVID-19 vaccination with dynamic social distancing. *Nature Human Behaviour, 6*, 193–206. https://doi.org/10.1038/s41562-021-01281-8
Martcheva, M. (2009). A non-autonomous multi-strain SIS epidemic model. *Journal of Biological Dynamics, 3*, 235–251. https://doi.org/10.1080/17513750802638712
Martcheva, M. (2013). *An introduction to mathematical epidemiology*. Springer International Publishing.
Ma, W., Takeuchi, Y., Hara, T., & Beretta, E. (2002). Permanence of an SIR epidemic model with distributed time delays. *Tohoku Mathematical Journal, 54*, 581–591. https://doi.org/10.2748/tmj/1113247650
Meskaf, A., Khyar, O., Danane, J., & Allali, K. (2020). Global stability analysis of a two-strain epidemic model with non-monotone incidence rates. *Chaos, Solitons & Fractals, 133*, Article 109647. https://doi.org/10.1016/j.chaos.2020.109647
M, M., Nuño, C. C.-C. M., & Feng, Z. (2005). Dynamics of two-strain influenza with isolation and partial cross-immunity. *SIAM Journal on Applied Mathematics, 65*, 964–982. https://doi.org/10.1137/S003613990

Nakata, Y., & Omori, R. (2015). Delay equation formulation for an epidemic model with waning immunity: An application to mycoplasma pneumoniae. *IFAC-PapersOnLine, 28*, 132–135. https://doi.org/10.1016/j.ifacol.2015.11.024
Nastasi, G., Perrone, C., Taffara, S., & Vitanza, G. (2022). A time-delayed deterministic model for the spread of COVID-19 with calibration on a real dataset. *Mathematics, 10*, 1–14. https://doi.org/10.3390/math10040661
Niño-Torres, D., Ríos-Gutiérrez, A., Arunachalam, V., Ohajunwa, C., & Seshaiyer, P. (2022). Stochastic modeling, analysis, and simulation of the COVID-19 pandemic with explicit behavioral changes in bogotá: A case study. *Infectious Disease Modelling, 7*, 199–211. https://doi.org/10.1016/j.idm.2021.12.008
Ogilvy Kermack, W., & McKendrick, A. G. (1927). A contribution to the mathematical theory of epidemics. *Proc. R. Soc. A Math. Phys. Eng. Sci., 115*, 700–721. https://doi.org/10.1098/rspa.1927.0118
Poletti, P., Caprile, B., Ajelli, M., Pugliese, A., & Merler, S. (2009). Spontaneous behavioural changes in response to epidemics. *Journal of Theoretical Biology, 260*, 31–40. https://doi.org/10.1016/j.jtbi.2009.04.029
Rajib Arefin, M., Masaki, T., Ariful Kabir, K. M., & Tanimoto, J. (2019). Interplay between cost and effectiveness in influenza vaccine uptake: A vaccination game approach. *Proc. R. Soc. A Math. Phys. Eng. Sci., 475*. https://doi.org/10.1098/rspa.2019.0608
Rihan, F. A., Alsakaji, H. J., & Rajivganthi, C. (2020). Stochastic SIRC epidemic model with time-delay for COVID-19. *Advances in Differential Equations*, 2020. https://doi.org/10.1186/s13662-020-02964-8
Szolnoki, A., & Perc, M. (2015). Conformity enhances network reciprocity in evolutionary social dilemmas. *Journal of the Royal Society Interface, 12*, 2–9. https://doi.org/10.1098/rsif.2014.1299
Tanimoto, J. (2015). *Fundamentals of evolutionary game theory and its applications*. Tokyo): Springer.
Tanimoto, J. (2019). *Evolutionary games with sociophysics: Analysis of traffic flow and epidemics*. Tokyo): Springer.
Tanimoto, J. (2021). *Sociophysics approach to epidemics*. Tokyo): Springer.
Tchoumi, S., & Tchuenche, J. M. (2021). Dynamic of a two-strain COVID-19 model with vaccination vaccination. *Research Square*, 1–15. https://doi.org/10.21203/rs.3.rs-553546/v1
Theprungsimankul, P., Junsank, S., Abdulloh, A., & Chinviriyasit, W. (2011). The effect of cross-immunity in a multi-strain epidemic model. *Kasetsart Journal, 45*, 563–570.
Tiwari, P. K., Rai, R. K., Khajanchi, S., Gupta, R. K., & Misra, A. K. (2021). Dynamics of coronavirus pandemic: Effects of community awareness and global information campaigns. *European Physical Journal - Plus, 136*. https://doi.org/10.1140/epjp/s13360-021-01997-6
Tori, R., & Tanimoto, J. (2022). A study on prosocial behavior of wearing a mask and self-quarantining to prevent the spread of diseases underpinned by evolutionary game theory. *Chaos, Solitons & Fractals, 158*, Article 112030. https://doi.org/10.1016/j.chaos.2022.112030
Xia, W., Kundu, S., & Maitra, S. (2018). Dynamics of a delayed SEIQ epidemic model. *Advances in Difference Equations. 2018*. https://doi.org/10.1186/s13662-018-1791-8
Yang, J., Chen, Y., & Liu, J. (2016). Stability analysis of a two-strain epidemic model on complex networks with latency. *Discrete and Continuous Dynamical Systems - Series B, 21*, 2851–2866. https://doi.org/10.3934/dcdsb.2016076
Yang, J., & Zhang, F. (2012). Stability of a two-strain epidemic model with an age structure. *Journal of Applied Mathematics and Informatics, 30*, 183–200.
Yin, Q., Wang, Z., Xia, C., & Bauch, C. T. (2022). Impact of co-evolution of negative vaccine-related information, vaccination behavior and epidemic spreading in multilayer networks. *Communications in Nonlinear Science and Numerical Simulation, 109*, Article 106312. https://doi.org/10.1016/j.cnsns.2022.106312
Zuo, C., Zhu, F., & Ling, Y. (2022). Analyzing COVID-19 vaccination behavior using an SEIRM/V epidemic model with awareness decay. *Frontiers in Public Health, 10*, 1–12. https://doi.org/10.3389/fpubh.2022.817749
Zuo, C., Zhu, F., Meng, Z., Ling, Y., Zheng, Y., & Zhao, X. (2022). Analyzing the COVID-19 vaccination behavior based on epidemic model with awareness-information. *Infection, Genetics and Evolution, 98*, Article 105218. https://doi.org/10.1016/j.meegid.2022.105218